Low-cost ultra-thin broadband terahertz beam-splitter

Benjamin S.-Y. Ung,[1,*] **Christophe Fumeaux,**[1] **Hungyen Lin,**[1] **Bernd M. Fischer,**[1,2] **Brian W.-H. Ng,**[1] **and Derek Abbott**[1]

[1]*School of Electrical & Electronic Engineering, The University of Adelaide, SA 5005, Australia*

[2]*Institut Franco-Allemand de Recherches de Saint Louis, BP 70034, 68301 Saint Louis Cedex, France*

**bung@eleceng.adelaide.edu.au*

Abstract: A low-cost terahertz beam-splitter is fabricated using ultra-thin LDPE plastic sheeting coated with a conducting silver layer. The beam splitting ratio is determined as a function of the thickness of the silver layer—thus any required splitting ratio can be printed on demand with a suitable rapid prototyping technology. The low-cost aspect is a consequence of the fact that ultra-thin LDPE sheeting is readily obtainable, known more commonly as domestic *plastic wrap* or *cling wrap*. The proposed beam-splitter has numerous advantages over float zone silicon wafers commonly used within the terahertz frequency range. These advantages include low-cost, ease of handling, ultra-thin thickness, and any required beam splitting ratio can be readily fabricated. Furthermore, as the beam-splitter is ultra-thin, it presents low loss and does not suffer from Fabry-Pérot effects. Measurements performed on manufactured prototypes with different splitting ratios demonstrate a good agreement with our theoretical model in both P and S polarizations, exhibiting nearly frequency-independent splitting ratios in the terahertz frequency range.

OCIS codes: (300.6495) Spectroscopy, terahertz; (040.2235) Far infrared or terahertz; (230.1360) Beam splitters.

References and links

1. R. Bakunov, R. Mikhaylovskiy, M. Tani, and C. Que, "A structure for enhanced terahertz emission from a photoexcited semiconductor surface," Appl. Phys. B-Lasers Opt. **100**, 695–698 (2010).
2. B. Clough, J. Liu, and X.-C. Zhang, ""All air-plasma" terahertz spectroscopy," Opt. Lett. **36**(13), 2399–2401 (2011).
3. D. J. Cook and R. M. Hochstrasser, "Intense terahertz pulses by four-wave rectification in air," Opt. Lett. **25**(16), 1210–1212 (2000).
4. J. Dai, X. Xie, and X.-C. Zhang, "Terahertz wave amplification in gases with the excitation of femtosecond laser pulses," Appl. Phys. Lett. **91**(21), 211102 (2007).
5. J. A. Fülöp, L. Pálfalvi, G. Almási, and J. Hebling, "Design of high-energy terahertz sources based on optical rectification," Opt. Express **18**(12), 12311–12327 (2010).
6. M. C. Hoffmann and J. A. Fülöp, "Intense ultrashort terahertz pulses: generation and applications," J. Phys. D-Appl. Phys. **44**(8), 083001 (2011).
7. P. U. Jepsen, D. Cooke, and M. Koch, "Terahertz spectroscopy and imaging—Modern techniques and applications," Laser Photon. Rev. **5**(1), 124–166 (2011).
8. K. Kawase, S. Ichino, K. Suizu, and T. Shibuya, "Half cycle terahertz pulse generation by prism-coupled Cherenkov phase-matching method," J. Infrared Millim. Terahertz Waves **32**, 1168–1177 (2011).

#161066 - $15.00 USD Received 6 Jan 2012; revised 3 Feb 2012; accepted 3 Feb 2012; published 13 Feb 2012

9. A. K. Malik, H. K. Malik, and S. Kawata, "Investigations on terahertz radiation generated by two superposed femtosecond laser pulses," J. Appl. Phys. **107**(11), 113105 (2010).
10. K. Reimann, "Table-top sources of ultrashort THz pulses," Rep. Prog. Phys. **70**(10), 1597 (2007).
11. A. M. Weiner, A. M. Kan'an, and D. E. Leaird, "High-efficiency blue generation by frequency doubling of femtosecond pulses in a thick nonlinear crystal," Opt. Lett. **23**(18), 1441–1443 (1998).
12. X. Xie, J. Xu, J. Dai, and X.-C. Zhang, "Enhancement of terahertz wave generation from laser induced plasma," Appl. Phys. Lett. **90**(14), 141104 (2007).
13. N. Zhong, N. Karpowicz, and X.-C. Zhang, "Terahertz emission profile from laser-induced air plasma," Appl. Phys. Lett. **88**(26), 261103-3 (2006).
14. C. Berry and M. Jarrahi, "Broadband terahertz polarizing beam splitter on a polymer substrate," J. Infrared Millim. Terahertz Waves **32**(12), 1–4 (2011).
15. C. C. Homes, G. L. Carr, R. P. S. M. Lobo, J. D. LaVeigne, and D. B. Tanner, "Silicon beam splitter for far-infrared and terahertz spectroscopy," Appl. Opt. **46**, 7884–7888 (2007).
16. J.-S. Li, D.-G. Xu, and J.-Q. Yao, "Compact terahertz wave polarizing beam splitter," Appl. Opt. **49**(24), 4494–4497 (2010).
17. Y. H. Lo and R. Leonhardt, "Aspheric lenses for terahertz imaging," Opt. Express **16**(20), 15991–15998 (2008).
18. B. Scherger, C. Jördens, and M. Koch, "Variable-focus terahertz lens," Opt. Express **19**(5), 4528–4535 (2011).
19. B. Scherger, M. Scheller, C. Jansen, M. Koch, and K. Wiesauer, "Terahertz lenses made by compression molding of micropowders," Appl. Opt. **50**(15), 2256–2262 (2011).
20. A. Siemion, A. Siemion, M. Makowski, M. Sypek, E. Hrault, F. Garet, and J.-L. Coutaz, "Off-axis metallic diffractive lens for terahertz beams," Opt. Lett. **36**(11), 1960–1962 (2011).
21. B. Voisiat, A. Bičiūnas, I. Kašalynas, and G. Račiukaitis, "Band-pass filters for THz spectral range fabricated by laser ablation," Appl. Phys. A-Matt. Sci. Process. **104**(3), 953-958 (2011).
22. S. Atakaramians, S. Asfar V., M. Nagel, H. K. Rasmussen, O. Bang, T. M. Munro, and D. Abbott, "Direct probing of evanescent field characterization of porous fibers," Appl. Phys. Lett. **98**(12), 121104 (2011).
23. R. Mendis and D. M. Mittleman, "Comparison of the lowest-order transverse-electric (TE1) and transverse-magnetic (TEM) modes of the parallel-plate waveguide for terahertz pulse applications," Opt. Express **17**(17), 14839–14850 (2009).
24. K. Nielsen, H. K. Rasmussen, A. J. Adam, P. C. Planken, O. Bang, and P. U. Jepsen, "Bendable, low-loss Topas fibers for the terahertz frequency range," Opt. Express **17**(10), 8592–8601 (2009).
25. B. Scherger, M. Scheller, N. Vieweg, S. T. Cundiff, and M. Koch, "Paper terahertz wave plates," Opt. Express **19**(25), 24884–24889 (2011).
26. C. Rønne, L. Thrane, P.-O. Åstrand, A. Wallqvist, K. V. Mikkelsen, and S. R. Keiding, "Investigation of the temperature dependence of dielectric relaxation in liquid water by THz reflection spectroscopy and molecular dynamics simulation," J. Chem. Phys. **107**, 5319 (1997).
27. S. A. Maier, *Plasmonics: Fundamentals and Applications* (Springer, 2007).
28. N. Laman, and D. Grischkowsky, "Terahertz conductivity of thin metal films," Appl. Phys. Lett. **93**(5), 051105 (2008).
29. D. G. Cooke, F. A. Hegmann, E. C. Young, and T. Tiedje, "Electron mobility in dilute GaAs bismide and nitride alloys measured by time-resolved terahertz spectroscopy," Appl. Phys. Lett. **89**, 122103 (2006).
30. F. A. Hegmann, O. Ostroverkhova, and D. G. Cooke, *Probing Organic Semiconductors with Terahertz Pulses Photophysics of Molecular Materials* (Wiley-VCH Verlag GmbH & Co. KGaA, 2006).
31. M. Tinkham, "Energy gap interpretation of experiments on infrared transmission through superconducting films," Phys. Rev. **104**, 845–846 (1956).
32. M. Walther, D. G. Cooke, C. Sherstan, M. Hajar, M. R. Freeman, and F. A. Hegmann, "Terahertz conductivity of thin gold films at the metal-insulator percolation transition," Phys. Rev. B **76**, 125408 (2007).
33. S. Bauer, "Optical properties of a metal film and its application as an infrared absorber and as a beam splitter," Am. J. Phys. **60**, 257–261 (1992).
34. M. Born and E. Wolf, *Principles of Optics* (Cambridge University Press, 1997).
35. O. S. Heavens, *Optical Properties of Thin Solid Films* (Butterworth's Scientific Publications, 1955).
36. M. Heald and J. Marion, *Classical Electromagnetic Radiation* (Brooks Cole, 1994).
37. M. Theuer, R. Beigang, and D. Grischkowsky, "Highly sensitive terahertz measurement of layer thickness using a two-cylinder waveguide sensor," Appl. Phys. Lett. **97**(7), 071106 (2010).

1. Introduction

With the continuous increase in power generated by terahertz (0.1 to 10 THz) radiation sources [1–13] and the progress of optical components, such as beam-splitters [14–16], lenses [17–20], filters [21] and waveguides [22–25], which operate at these frequencies, there is a need for beam-splitters that provide small dispersion, low absorption and minimize Fabry-Pérot effects.

#161066 - $15.00 USD Received 6 Jan 2012; revised 3 Feb 2012; accepted 3 Feb 2012; published 13 Feb 2012

Further qualities of the beam-splitter should include; accurate setting of the ratio of reflected and transmitted power, minimal time-domain distortion of terahertz pulses and minimal beam deviation of the transmitted path. This paper proposes a beam-splitter that satisfies these criteria and is fabricated from low cost materials, in a scalable fabrication process.

Currently, beam-splitters for terahertz frequencies are often fabricated from high impedance silicon (Hi-Z Si) wafers [15], where a given splitting ratio cannot be rapidly manufactured on demand. Moreover, silicon wafers suffer from frequency-dependent oscillations arising from Fabry-Pérot effects. Other beam-splitters meanwhile are polarization dependent [14, 16], are again restricted to limited splitting ratios, or delay the transmitted time-domain pulse, which limits their application range.

The proposed ultra-thin LDPE (low density polyethylene) beam-splitter is based on the partial transmission through a very thin conducting film. Any given splitting ratio can be obtained during fabrication selecting the correct thickness for the thin-metal coating on the top of the ultra-thin LDPE substrate. The ultra-thin LDPE sheets are typically manufactured for domestic use to a thickness of 6.5 μm. This simple arrangement does not distort time-domain pulses due to its very small overall thickness. The properties of the thin-metal film are determined by a reflection from a thin conductive layer below the skin depth at terahertz frequencies, as explained in more detail in Section 2. This beam-splitter may potentially provide an alternative for those used in reflection mode Terahertz Time-Domain Spectroscopy (THz-TDS) systems [26], high powered terahertz systems that can accommodate several beams to power multiple systems, and also for quantum cascade lasers, where a diagnostic sample of the beam may be required for real-time monitoring.

This paper discusses the theoretical model for the thin-film conductor coating, the fabrication technique, experimental methods to measure and characterize samples, and comments on the results achieved with samples of differing thicknesses. A comparison of the prototypes with commonly used Hi-Z Si wafers will conclude the paper.

2. Theoretical model

Conventional beam-splitters for terahertz applications rely on the partial reflection arising from the dielectric contrast at material interfaces. Broadband applications preclude the use of $\frac{\lambda}{4}$ interference coatings to achieve a better control over the partial reflection and transmission ratio. In contrast to the traditional dielectric terahertz beam-splitters, the proposed beam-splitter is based on reflection from a thin metal coating applied to the surface of an ultra-thin dielectric LDPE substrate. To model this arrangement, we consider a thin conductive layer, with a complex index of refraction and finite conductivity. It is also necessary to estimate the skin depth required at terahertz frequencies, as a substantial amount of transmission will only be possible for conductor thicknesses below the skin depth. The skin depth δ can be calculated [27] as

$$\delta = \sqrt{\frac{2}{\mu_0 \mu_r \sigma_0 \omega}}, \tag{1}$$

where μ_0 is the magnetic permeability of free space, σ_0 is the DC conductivity, μ_r is the relative permeability of the medium and ω is the angular frequency.

For the silver conductive paint used in this paper, the skin depth calculated in the range of frequencies from 0.1 to 3.5 THz decreases from approximately 72 to 12 μm, using values of $\mu_r = 1$ and $\sigma_0 = 500$ S·m^{-1} (this value will be discussed later in Section 5). As it is possible to fabricate the beam-splitters with coatings below these thicknesses, the transmissive properties can be accurately determined. For a theoretical calculation of the relative transmission of the metallic coating, with respect to thickness and frequency, the Tinkham formula [29–32] can be used

#161066 - $15.00 USD Received 6 Jan 2012; revised 3 Feb 2012; accepted 3 Feb 2012; published 13 Feb 2012

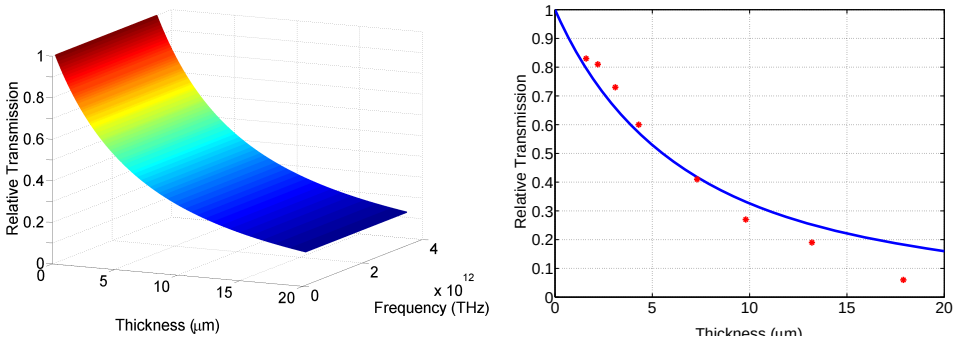

(a) (b)

Fig. 1. (a) A plot of thickness and frequency against relative transmission. The transmission appears to be nearly invariant over the frequency range, due to the small layer thickness well below the skin depth. (b) Simplified frequency-invariant model of transmission dependent only on the thickness of the paint. The blue curve is plotted according to the theoretical model and fitted with a DC conductivity of 500 S·m^{-1}, while the red points represent the measured data.

$$T(\omega) = \left| \frac{E_{\text{sample}}(\omega)}{E_{\text{reference}}(\omega)} \right| = \frac{1}{\left| 1 + \tilde{\sigma} d \cdot \frac{Z_0}{n_{\text{substrate}}+1} \right|^2}, \tag{2}$$

where $T(\omega)$ is the transmission calculated with respect to frequency, $\tilde{\sigma}$ is the complex conductivity of the metal, d is the thickness of the metallic layer, $n_{\text{substrate}}$ is the refractive index of the substrate and Z_0 is the impedance of free space.

The dispersion of the complex conductivity $\tilde{\sigma} = \sigma_1 + j\sigma_2$, is calculated as

$$\sigma_1 = \frac{\sigma_0}{1+(\omega\tau)^2}, \quad \sigma_2 = \sigma_0 \cdot \frac{-(\omega\tau)}{1+(\omega\tau)^2}, \quad \text{with,} \quad \tau = \frac{m_0 \sigma_B}{Ne^2}, \tag{3}$$

where m_0 is the electron rest mass, σ_B is Stefan-Boltzman constant, N is the free electron density, e is the electron volt charge and τ is the damping time constant [27].

Using a LDPE substrate, which has a constant refractive index of n = 1.51 from lower terahertz frequencies up to 5 THz, and silver conductive paint as the metallic layer, the relationship between the thickness and the relative transmission for all frequencies in the considered range can be calculated using Eq. (2). The result of this computation is shown in Fig. 1a for silver paint thicknesses between 0 and 20 μm, in the frequency range of 0.1 to 3.5 THz. Of particular note, it is observed that the relative transmission calculated from the given frequency range shows that transmission is in fact nearly frequency independent for very thin conductive layers, which follows the calculations by Walther et al. [32]. Therefore, the frequency dependence can be removed from the considerations to simplify the model. This results in a transmission dependence based only on the thickness, as plotted in Fig. 1b. This plot shows that in order to obtain a 50:50 ratio of reflection to transmission, a metallic coating of approximately 5.5 μm would need to be obtained assuming a DC conductivity of 500 S·m^{-1}. Other ratios can be similarly determined from this data. It is noted that this approximation does not take into account absorption from the thin substrate.

The presented theoretical model has so far only considered the case of normal incidence. For practical scenarios, the beam-splitter might need to be placed at different angles of incidence,

#161066 - $15.00 USD Received 6 Jan 2012; revised 3 Feb 2012; accepted 3 Feb 2012; published 13 Feb 2012

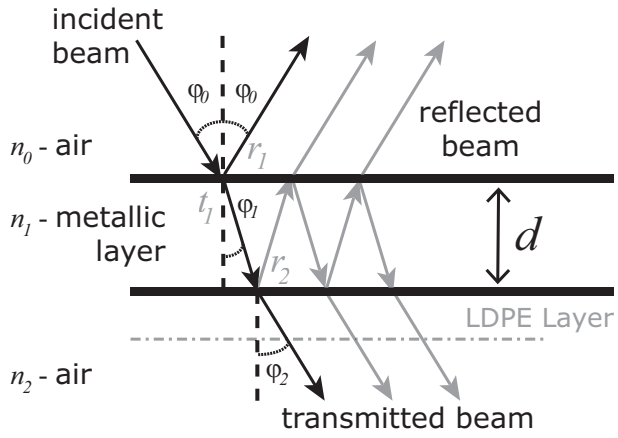

Fig. 2. Schematic diagram of the Fabry-Pérot effect in the layers of the beam-splitter. The very thin LDPE layer can be neglected here as it does not exhibit any measurable time delay or losses at terahertz frequencies. The Fresnel coefficients used in Eq. (4) are denoted here by t_1, r_1 and r_2.

for example 45° degrees in interferometric applications. This requires the use of Fabry-Pérot equations [33–36] for determining the angular dependence for the reflectance and transmittance of beam-splitter samples at varying angles of incidence. To set-up these equations, the first medium where the beam is incident is air, the second medium is the silver conductive paint, followed by air again. The very thin low-permittivity substrate sheet of LDPE is ignored here, as it has negligible effects at terahertz frequencies. The arrangement is shown in Fig. 2, where air, silver conductive paint and air are denoted by the subscripts, 0, 1 & 2 respectively and δ_1 is the phase delay between media. The reflectance can be calculated by

$$R = r_1 - t_1^2 r_2 e^{-2i\delta_1} + t_1^2 r_1 r_2^2 e^{-4i\delta_1} - t_1^2 r_1^2 r_2^3 e^{-6i\delta_1} + \ldots \tag{4}$$

Standard Fresnel coefficients t_1, r_1 and r_2 in Eq. (4) are defined in Fig. 2, can be calculated for both horizontal (P) and vertical (S) polarizations as given in Heavens [35] and $\delta_1 = (2\pi n_1 d_1 \cos\varphi_1)/\lambda$. The terms of the series after the third order can be neglected, due to the rapid convergence of the model.

The relative ratio A of power absorbed in the lossy paint, can be calculated from Bauer [33]

$$A = \frac{\frac{4y}{\tilde{n}}\cos\varphi_0}{(2+\frac{y}{\tilde{n}}\cos\varphi_0)^2}, \tag{5}$$

where $\tilde{n}$ is the complex refractive index of the silver conductive paint, $y = (\sigma_0 d)/(\varepsilon_0 c)$ with ε_0 the permittivity of vacuum and c the speed of light. Now, applying the conservation of energy, the theoretical transmittance can be calculated as

$$T = 1 - R - A. \tag{6}$$

The modeled T, R & A for both P and S polarizations will be compared to the measured data in the results section.

3. Fabrication

Low cost off-the-shelf materials are used for fabrication of the beam-splitter. Initially, a 50 mm inner diameter aluminum ring is fabricated as the frame structure for the beam-splitter. The

#161066 - $15.00 USD Received 6 Jan 2012; revised 3 Feb 2012; accepted 3 Feb 2012; published 13 Feb 2012

Fig. 3. Photograph of the fabricated beam-splitters. From the left, beam-splitters are shown with a terahertz reflection/transmission ratio of 10:90, 50:50 & 90:10. The expanded views show photos from a microscope camera showing the surface of the silver conductive paint layer at a magnification of 60×. These microscope photos show that the area of the LDPE is covered more than 10% and 50% for the 10:90 and 50:50 ratio beam-splitters respectively, demonstrating that they are not area based polka-dot beam-splitters.

substrate material used is common generic branded supermarket purchased LDPE cling-wrap, with a thickness of approximately 6.5 μm—this thickness is lower than that of Theuer et al. [37] as the LDPE is stretched over the aluminum ring. This low cost material presents a low terahertz absorption and is relatively easy to handle. The aluminum ring is heated in an oven for 5 minutes at a temperature of 160°C. The LDPE sheet is stretched over the ring, and slightly melts thereby forming a bond onto the metal surface. The ring is allowed to return to room temperature in a minimal dust environment. The ring with the LDPE sheet is weighed to provide a reference point. Common silver paint (Electrolube ESCP03B) is thinned out using ethanol to obtain sufficiently small paint droplets. This mixture is then placed into an airbrush with a minimum nozzle size of 200 μm, and sprayed at an arm's length to the stretched LDPE sheet, providing a uniform coverage (fabricated samples are shown in Fig. 3). The paint is allowed to dry at room temperature for 30 minutes and the ring with coated sheet is weighed again. The increase in weight from the initial value of weight is then used to determine the thickness of the layer of paint applied to the beam-splitter, given the known density. Optical profilometry (Ambios Profilometer) is used to check the density, thickness, uniformity and surface roughness of the coatings, providing confidence that all calculations are accurate. The optical profilometry shows that samples have good uniformity of with a standard deviation of approximately 1.7 μm for a sample with average conductive silver paint thickness 9.8 μm. The average value of the thickness in this case shows good accordance with the calculated values based on paint density, area and weight difference.

The paint shows good adhesion with the LDPE film, requiring targeted damage to scratch the paint from the surface. Moreover, the LDPE film requires significant force to dislodge it from the aluminum ring. With due care, the conductive paint coating has remained intact for over 6 months.

4. Experimentation

The experimental set-up for the measurement of transmittance and reflectance from the beam-splitter for incidence is performed with a Picometrix T-Ray 2000XP THz-TDS system as shown in Fig. 4. This system is advantageous as the fibers coupled to the emitter and detector heads

#161066 - $15.00 USD Received 6 Jan 2012; revised 3 Feb 2012; accepted 3 Feb 2012; published 13 Feb 2012

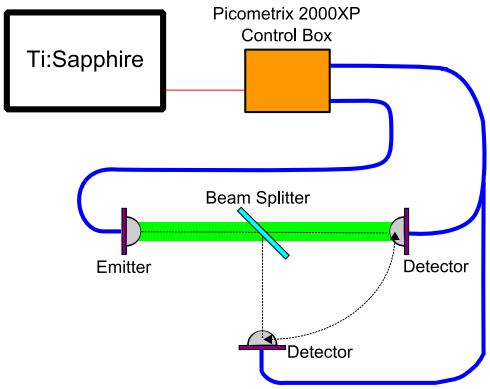

Fig. 4. Schematic diagram of the Picometrix 2000XP THz-TDS system. The output of a Ti:Sapphire laser (Spectra-Physics Mai-Tai with a pulse-width of <100 fs) is coupled into the control box of the Picometrix 2000XP system which is fiber-coupled to movable emitter and detector heads, allowing transmission and reflection from the beam-splitter to be be measured for varying angles of incidence.

enable them to be moved around an optical table freely, thus permitting measurements to be conducted at varying angles of incidence. The limitation of the system however does not allow reflection measurements to be performed at normal incidence. Therefore, as an exception, a reflection based THz-TDS [26] has been used for this particular case.

An initial measurement on an uncoated LDPE film confirmed that this layer can be neglected. Coated samples were then measured to characterize their transmission and reflection profiles. The measurements were performed in air atmosphere for angles of incidence φ_0 varying from 25° to 50° in both P and S polarizations. Transmission measurement of a 9.8 μm coated sample at normal incidence demonstrate that the transmitted pulse is attenuated compared to the reference pulse, however without any delay in the time-domain pulse (Fig. 5a) or added spectral features on the frequency curve (Fig. 5b).

5. Results

Data is obtained from transmitted pulses of multiple beam-splitter samples at normal incidence and are plotted in comparison with the modeled data in Fig. 1b. This measured data is curve-fitted to the theoretical model of Eq. (2) (Fig. 1b), yielding the DC conductivity of the silver conductive paint of $\sigma_0 = 500\ \mathrm{S{\cdot}m^{-1}}$, this DC conductivity is much lower than that of Laman et al. [28], due to the difference between the silver conductive paint and pure metal. This value fits the data to a correlation factor of $R = 0.9965$, showing close conformity to the curve fitted DC conductivity. The discrepancy between the model and the measurements observed for the thinnest and thickest samples are attributed to the effects related to the uniformity of the paint layers: Non-uniformities, which are more pronounced for thinner layers, tend to decrease the conductivity of the film. It can be observed in the microscope photographs shown, as insets in Fig. 3, that the paint particles become more densely joined together as the thickness increases.

Measurement data for the transmittance at normal incidence are presented in Fig. 6 for beam-splitters fabricated for different splitting ratios averaged over the frequency range of 0.5 to 1.5 THz. The ratios of reflectance to transmittance are varied in steps from approximately 10:90 to 90:10. An interesting observation is that, as the frequency decreases and the thick-

#161066 - $15.00 USD Received 6 Jan 2012; revised 3 Feb 2012; accepted 3 Feb 2012; published 13 Feb 2012

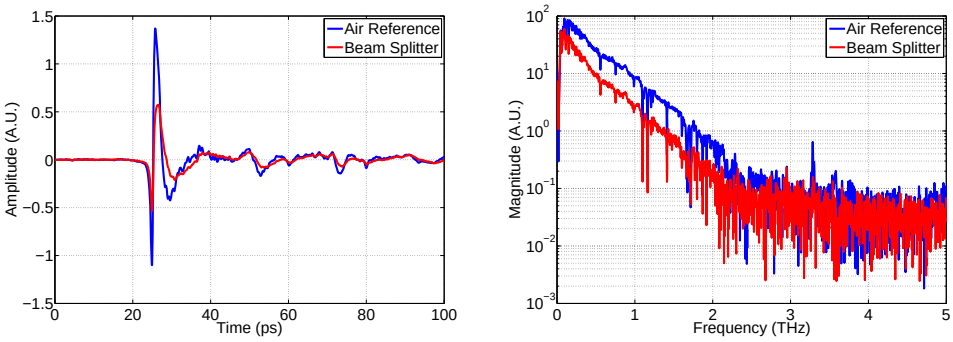

(a) (b)

Fig. 5. (a) Time-domain of the reference pulse and LDPE beam-splitter in lab air. The shape of the time-domain pulse is not affected by the transmission through the beam-splitter. (b) Frequency plot of the reference pulse and of the pulse transmitted through the beam-splitter. The beam-splitter does not contribute additional absorption peaks, while the broadband attenuation appears to be approximately uniform. The splitting ratio of the beam-splitter used here is 60:40.

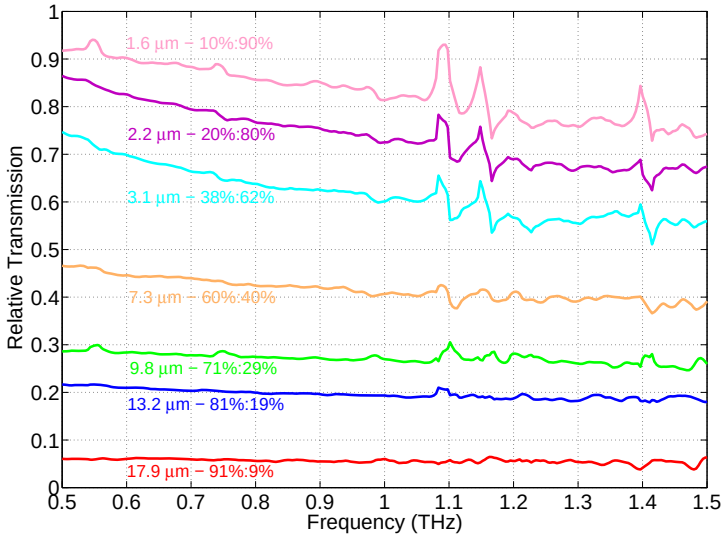

Fig. 6. Terahertz transmission plots of beam-splitters with varying thickness at normal incidence. The increase in the conductive layer thickness led to decreased transmission. The peaks in the curves are due to the water absorption in lab air. The modelled values of splitting ratios are depicted next to each curve.

#161066 - $15.00 USD Received 6 Jan 2012; revised 3 Feb 2012; accepted 3 Feb 2012; published 13 Feb 2012

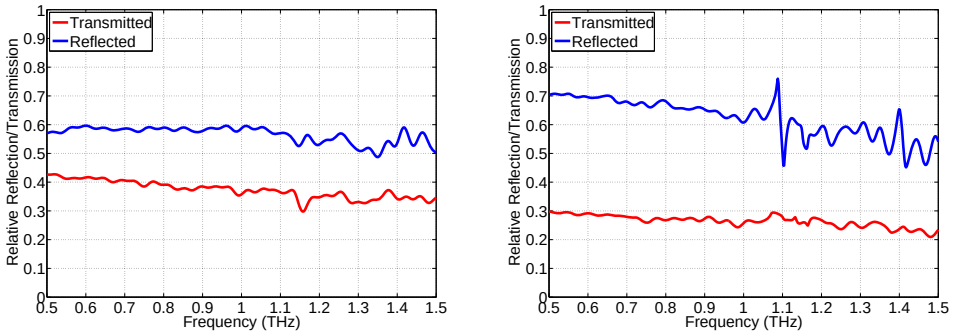

(a) (b)

Fig. 7. (a) and (b) P and S polarization plots of relative reflection and transmission of a beam-splitter with splitting ratio of 60:40 at 45° incidence. It can be noted that the P polarization reflectance (a) is lower than that of the S polarization (b) in agreement with the modelled results shown in Figs. 8a & 8b.

ness approaches one fifth of the skin depth (approximately 0.8 THz), higher transmission can be observed. This is consistent with the work presented by Walther et al. [32], where thinner metal films exhibited higher relative transmission than the theoretical model used due to the lower conductivity arising from the mentioned inhomogeneities. The thicker coatings in contrast, show fewer voids, and thus exhibit a higher conductivity closer to the quoted DC conductivity of the silver conductivity paint. Back calculations from the data show that the conductivity drops to 150 $S{\cdot}m^{-1}$ for the thinner coatings from 500 $S{\cdot}m^{-1}$ of the thicker coatings.

The measurements for 45° incidence are shown in Figs. 7a & 7b only for a specific sample for brevity. These curves illustrate the behaviour of the beam-splitters at 45° in both polarizations, and as expected, do not exhibit a strong frequency dependence. The selected sample has an approximate thickness of 9.8 μm and a modelled splitting ratio of approximately 60:40 reflection to transmission. Due to the physical constraints of the system and to the finite size of the beam-splitter's aperture, the angular range is limited to φ_0 equaling 25° to 50° for both reflection and transmission. The experimental results at 1 THz are plotted in Figs. 8a & 8b for the polarizations P and S respectively. A close agreement of the experimental data with the theoretical model is observed in both polarizations. In particular, an increase in transmittance is observed in Fig. 8a, as the angle of incidence increases towards the Brewster angle of the silver conductive paint, at 72°. In contrast for the S polarization, a steady increase in reflectance is observed together with a decrease in the transmittance as the angle of incidence increases. The estimated losses in both polarizations are also consistent with the error range calculated from the standard deviation of the thickness of the silver conductive paint (in this case approximately ±5.5%). For both polarizations, the efficiency at 1 THz of the beam-splitter is approximately 90%.

6. Comparison with dielectric beam-splitters

Commonly, Hi-Z Si wafers are employed in THz-TDS systems as beam-splitters [15]. The frequency-dependent performance of two such beam-splitters with different thicknesses (200 μm and 1 mm) have been measured for comparison with the proposed thin-metal-film beam-splitter. The results are plotted in Fig. 9 and show that Hi-Z Si wafers (without time-domain echos removed), suffer greatly from strong frequency-dependent oscillations of the

#161066 - $15.00 USD Received 6 Jan 2012; revised 3 Feb 2012; accepted 3 Feb 2012; published 13 Feb 2012

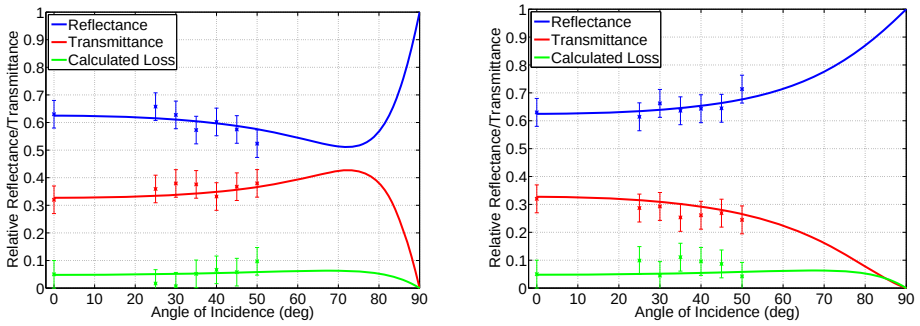

Fig. 8. (a) Relative transmission, reflection and loss in P polarization. (b) Relative transmission, reflection and loss in S polarization. The error bars in (a) and (b) are calculated from the standard deviation of the thickness of coatings for a sample with a beam-splitting ratio of 60:40. The solid lines denote the model used, while the points show the measured data.

splitting ratio, arising from Fabry-Pérot interference effects. This is particularly critical for thicker samples, whereas it can be noted that the thinner sample exhibits slower oscillations, but is difficult to handle. Removing the interferences through time-gating requires thick samples, which are bulky and expensive. For a similar averaged ratio of reflection to transmission, the proposed thin conductive film beam-splitter has a much smoother transmission curve and avoids Fabry-Pérot interference effects, due to the low refractive index and very thin substrate. An additional advantage of the thin-metal-film beam-splitters are that the ratios of reflection and transmission can be adjusted and optimized for particular systems unlike the fixed ratio provided by Hi-Z Si.

7. Potential improvements

To increase the accuracy of ratio adjustment and minimize surface roughness of the silver conductive paint layer, adjustments during fabrication could be implemented. A possible method for this fabrication would be to replace spray coating by inkjet printing, thus providing a means for rapid prototyping. In that case, accurately sized droplets of the silver paint can be deposited layer by layer to achieve the desired thickness. This controlled stepping would allow for a more controlled surface roughness, making for greater precision in setting the beam splitting ratio.

8. Conclusion

A low cost ultra-thin LDPE beam-splitter has been presented for low-dispersion splitting for reflection and transmission in THz-TDS systems. Several fabricated samples have been characterized physically and optically, and the transmission/reflection properties have been compared to a theoretical model. In addition, the angular characteristics for practical applications of the beam-splitter have been demonstrated at both horizontal and vertical polarizations. Finally, the performance of this beam-splitter has been compared to the traditionally used Hi-Z Si wafers. Potential applications for this beam-splitter include a beam-sampler for real-time monitoring of high-power sources, as well as a potential replacement for Hi-Z Si wafers in reflection mode terahertz spectroscopy systems or in operating at terahertz frequencies.

#161066 - $15.00 USD Received 6 Jan 2012; revised 3 Feb 2012; accepted 3 Feb 2012; published 13 Feb 2012

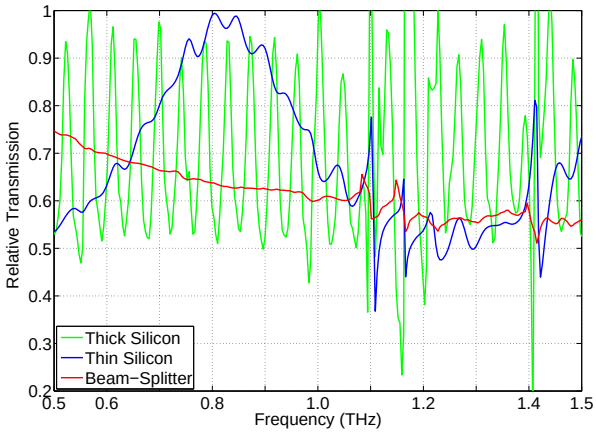

Fig. 9. Comparison of the transmittance curves for a 1 mm thick Hi-Z Si wafer (green), a thin 200 μm wafer (blue) and a silver painted beam-splitter with a splitting ratio of 38:62. Note that the LDPE beam-splitter exhibits a smoother transmission as a function of frequency, compared to the two Hi-Z Si wafers without Fabry-Pérot interference being removed within the time-domain.

Acknowledgments

Thanks are due to Alban O'Brien for technical assistance in manufacture. Withawat Withayachumnankul is gratefully acknowledged for technical discussions and Charan Shah for technical assistance with the optical profilometry. Support from the Australian Research Council (ARC) is gratefully acknowledged under Discovery Projects DP120100661, DP1097281, and DP0988673. Hungyen Lin acknowledges the D R Stranks Travelling Fellowship.